



Cite this: *Dalton Trans.*, 2014, **43**, 14409

Donor-activated alkali metal dipyridylamides: co-complexation reactions with zinc alkyls and reactivity studies with benzophenone†‡

David R. Armstrong, Etienne V. Brouillet, Alan R. Kennedy, Jennifer A. Garden,* Markus Granitzka, Robert E. Mulvey* and Joshua J. Trivett

Previously it was reported that activation of ${}^t\text{Bu}_2\text{Zn}$ by $[(\text{TMEDA})\text{Na}(\mu\text{-dpa})]_2$ led to *tert*-butylation of benzophenone at the challenging *para*-position, where the sodium amide functions as a metalloligand towards ${}^t\text{Bu}_2\text{Zn}$ manifested in crystalline $[(\text{TMEDA})\text{Na}(\text{dpa})]_2\text{Zn}^t\text{Bu}_2$ (TMEDA is *N,N,N',N'*-tetramethylethylenediamine, dpa is 2,2'-dipyridylamide). Here we find altering the Lewis donor or alkali metal within the metalloligand dictates the reaction outcome, exhibiting a strong influence on alkylation yields and reaction selectivity. Varying the former led to the synthesis of three novel complexes, $[(\text{PMDETA})\text{Na}(\text{dpa})]_2$, $[(\text{TMDAE})\text{Na}(\text{dpa})]_2$, and $[(\text{H}_6\text{-TREN})\text{Na}(\text{dpa})]$, characterised through combined structural, spectroscopic and theoretical studies [where PMDETA is *N,N,N',N',N''*-pentamethyldiethylenetriamine, TMDAE is *N,N,N',N'*-tetramethyldiaminoethylether and $\text{H}_6\text{-TREN}$ is *N',N'*-bis(2-aminoethyl)ethane-1,2-diamine]. Each new sodium amide can function as a metalloligand to generate a co-complex with ${}^t\text{Bu}_2\text{Zn}$. Reacting these new co-complexes with benzophenone proved solvent dependent with yields in THF much lower than those in hexane. Most interestingly, sub-stoichiometric amounts of the metalloligands $[(\text{TMEDA})\text{Na}(\text{dpa})]_2$ and $[(\text{PMDETA})\text{Na}(\text{dpa})]_2$ with 1 : 1, ${}^t\text{Bu}_2\text{Zn}$ –benzophenone mixtures produced good yields of the challenging 1,6-*tert*-butyl addition product in hexane (52% and 53% respectively). Although exchanging Na for Li gave similar reaction yields, the regioselectivity was significantly compromised; whereas the K system was completely unreactive. Replacing ${}^t\text{Bu}_2\text{Zn}$ with $(\text{Me}_3\text{SiCH}_2)_2\text{Zn}$ shut down the alkylation of benzophenone; in contrast, ${}^t\text{BuLi}$ generates only the reduction product, benzhydrol. Zincation of the parent amine dpa(H) generated the crystalline product $[\text{Zn}(\text{dpa})_2]$, as structurally elucidated through X-ray crystallography and theoretical calculations. Although the reaction mechanism for the alkylation of benzophenone remains unclear, incorporation of the radical scavenger TEMPO (2,2,6,6-tetramethylpiperidine-*N*-oxyl radical) into the reaction system completely inhibits benzophenone alkylation.

Received 27th March 2014,

Accepted 18th June 2014

DOI: 10.1039/c4dt00914b

www.rsc.org/dalton

Introduction

Derived from sterically imposing secondary amines (R_2NH), polar metal amides have a long successful track record as important reagents in synthesis, with several recent reviews confirming that their popularity continues to be high.^{1–6} Although in this category monometallic amides are well-established

components of the synthetic chemist's toolbox, current research has brought heterobimetallic amides into the limelight. The synergic combination of two metals within an organoamide-ligand environment has often led to unexpected and unprecedented chemistry, which cannot be reproduced by either metal acting in isolation. Sophisticated bimetallic bases have been developed, where perhaps counter intuitively, it is sometimes but not always the softer polyvalent metal (such as Zn ,^{7–9} Mg ,^{10,11} Al ,^{12,13} Cd ,^{14–16} or Mn ^{17,18}) that executes metallo-deprotonation (conversion of an inert C–H bond to a labile, more synthetically flexible C–metal bond), assisted by the presence of a reactivity enhancing alkali metal.

Amongst other types of bond forming reactions, alkylselective addition to ketones has been much studied using several different organometallic reagents, including polar metal amides.⁸ Benzophenone is often used as a benchmark ketone

WestCHEM, Department of Pure and Applied Chemistry, University of Strathclyde, Glasgow, G1 1XL, UK. E-mail: r.e.mulvey@strath.ac.uk

† Dedicated to the memory of Ken Wade FRS. A brilliant intuitive chemist, generous in his wisdom and time to all who asked for his advice. REM remembers with great affection his postdoctoral period with Ken.

‡ Electronic supplementary information (ESI) available: NMR spectroscopic data, computational details and X-ray data in crystallographic file (CIF) format for compounds 2, 3 and 6. CCDC 992383–992385. For ESI and crystallographic data in CIF or other electronic format see DOI: 10.1039/c4dt00914b

for assessing organometallic reagents as its reactions can have several potential outcomes.^{8,19–22} Monometallic reagents generally produce significantly greater proportions of the hydride reduction product benzhydrol [$\text{Ph}_2\text{C}(\text{H})\text{OH}$] (with $^n\text{BuMgCl}$; 56%, $^n\text{BuLi}$; 38%); whereas bimetallic combinations can offer superior selectivity, with the use of the synergic lithium magnesiate base $^n\text{Bu}_3\text{MgLi}\cdot\text{LiCl}$ leading to exclusive carbonyl (1,2-) addition in an impressive 95% yield.¹⁹ Selective alkylation at the more challenging *para* (1,6-) position has also been realised using a bimetallic reagent, in the structurally defined sodium amidozincate $[(\text{TMEDA})\text{Na}(\mu\text{-TMP})(\mu\text{-}^t\text{Bu})\text{Zn}(^t\text{Bu})]$ (where TMEDA is N,N,N',N' -tetramethylethylenediamine and TMP is 2,2,6,6-tetramethylpiperidine).^{8,23} Thus the identity of the organometallic reagent exerts a strong influence upon the reaction outcome.

In a recent communication we described how sub-stoichiometric quantities of the sodium amide, $[(\text{TMEDA})\text{Na}(\text{dpa})]_2$, can activate $^t\text{Bu}_2\text{Zn}$ (within the sodium–zinc compound $\{[(\text{TMEDA})\text{Na}(\text{dpa})]_2\text{Zn}^t\text{Bu}_2\}$, **1**, Fig. 1, where the sodium amide functions as a metalloligand) towards more improved alkylation of benzophenone in the *para*-position [where dpa is 2,2'-dipyridylamide, $(2\text{-NC}_5\text{H}_4)_2\text{N}^-$].²⁴ This intriguing result prompted us to ask various questions. Would changing the constituents of the metalloligand allow us to tune the reactivity and selectivity towards the alkylation of benzophenone? Is the coordination of TMEDA to sodium within the metalloligand structure important to the outcome of these addition reactions? Can we extend this system to sodium's nearest neighbours, lithium and potassium? Can the reaction scope be broadened to other alkyl groups? The studies reported herein aimed to find answers to these important questions. Thus, a range of alkali metal dipyridylamide metalloligands was applied to the alkylation of benzophenone, using $^t\text{Bu}_2\text{Zn}$ as the alkyl transfer reagent. Through the combination of spectroscopic and structural characterisation data backed up with theoretical calculations, this study sheds insight upon the impact of changing parameters such as the Lewis donor, alkali metal and solvent polarity upon the yields and product distribution.

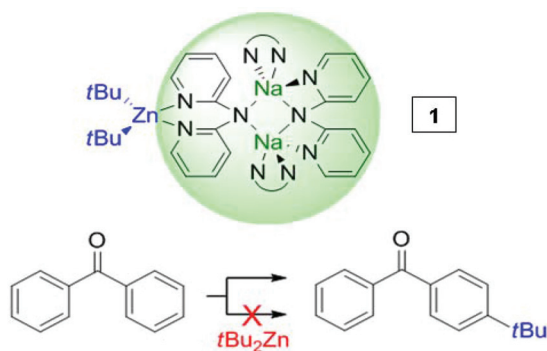


Fig. 1 The *tert*-butylation of benzophenone using $^t\text{Bu}_2\text{Zn}$ activated by a sodium amide metalloligand (top), in contrast to $^t\text{Bu}_2\text{Zn}$ alone which is ineffectual (bottom).

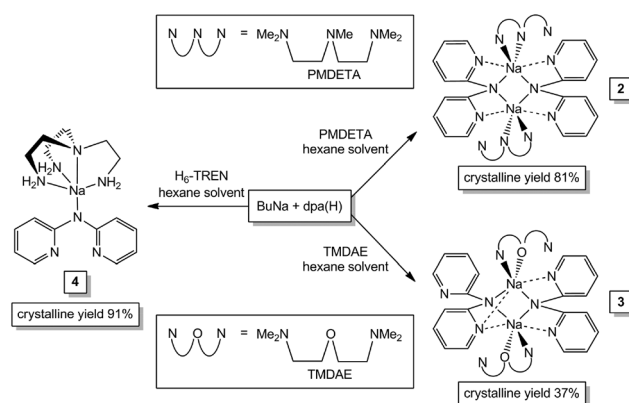
Results and discussion

Modification of the donor ligand: synthesis of a series of sodium dipyridylamide metalloligands

Striving to establish the importance or otherwise of the donor employed within the $[(\text{TMEDA})\text{Na}(\text{dpa})]_2$ metalloligand, we prepared a series of related sodium amide compounds with the general formula $[(\text{donor})\text{Na}(\text{dpa})]_x$. The alternative Lewis donors used were PMDETA (N,N,N',N',N' -pentamethyldiethylenetriamine), TMDAE (N,N,N',N' -tetramethyldiaminoethyl-ether) and $\text{H}_6\text{-TREN}$ [N,N' -bis(2-aminoethyl)ethane-1,2-diamine] (Scheme 1). We began by deprotonating the parent amine dpa(H) with *n*-butylsodium in hexane solvent. This reaction produced a white suspension. The mixture was subsequently treated with the appropriate donor amine. For the trifunctional donors PMDETA and TMDAE, two molar equivalents (on a 1 mmol scale reaction) were required to dissolve the suspension. Initially made up at ambient temperature, the reaction solutions were cooled to -30°C in order to grow poor quality crystals of $[(\text{PMDETA})\text{Na}(\text{dpa})]_2$ [**2**, 81% isolated yield (reported yields are based upon the dpa(H) stoichiometry)] and $[(\text{TMDAE})\text{Na}(\text{dpa})]_2$ [**3**, 37% yield] respectively. Upon moving to tetrafunctional $\text{H}_6\text{-TREN}$ (one molar equivalent), addition of toluene to the yellow-green oil and gentle heating produced a pale yellow solution, which upon gradual cooling to ambient temperature afforded a crop of colourless crystals of $[(\text{H}_6\text{-TREN})\text{Na}(\text{dpa})]$ (**4**) in a high isolated yield of 91%. New sodium amides **2–4** were characterised in solution using multinuclear (^1H , $^{13}\text{C}\{^1\text{H}\}$) NMR spectroscopy, and the molecular structures of **2** and **3** were elucidated by X-ray crystallographic studies.

Structural insights into sodium dipyridylamides **2–4**

Unfortunately, twinning, disorder and weak diffraction leads to a sub-optimal structural solution of **2**, which prevents any discussion of its dimensions (see the ESI† for a geometry-optimised model, **2**_{calc}, using DFT calculations). However, its atomic connectivity can be discerned (Fig. 2). Adopting a commonly observed motif within alkali metal chemistry,^{25,26} and



Scheme 1 Synthesis of sodiated dipyridylamine dimers **2** and **3**, and monomer **4**.

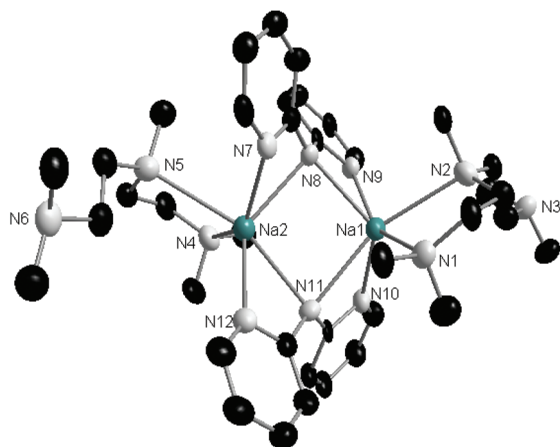


Fig. 2 Molecular structure of **2** with thermal ellipsoids at 50% probability level and hydrogen atoms and disordered components omitted for clarity.

most pertinently for sodium amides^{27–29} such as $[(\text{TMEDA})\text{Na}(\text{NPh}_2)_2]^{28}$ and $[(\text{THF})\text{Na}(\text{HMDS})_2]^{30}$ **2** adopts a dimeric, cyclic arrangement, where each Na centre is coordinated by two bridging dipyrildiamide units and a chelating PMDETA. An unusual feature is the incomplete chelation by the triamine donor PMDETA, which engages Na in a bidentate rather than in its common full tridentate capacity. ¹H NMR spectroscopic analysis of **2** suggests that this bidentate bonding mode is not retained in C_6D_6 solution (*vide infra*). A search of the CSD revealed only 11 structurally characterised compounds displaying this rare bidentate bonding mode, in comparison to 425 that involve tri-coordination of PMDETA to a Lewis acidic metal centre.³¹ Most relevant to **2** is the structurally related phenyl complex $[(\text{PMDETA})\text{Na}\{\text{Ph}(2\text{-NC}_5\text{H}_4)\text{N}\}]_2^{32}$ both possess a planar $[\text{NaNNa}]\text{N}$ ring core; with hexa-coordinated Na adopting a distorted octahedral geometry; and with two amido bridges connecting the two Na centres. However, a key distinction between the two structures is the bonding mode of the bridging amide unit. Within $[(\text{PMDETA})\text{Na}\{\text{Ph}(2\text{-NC}_5\text{H}_4)\text{N}\}]_2$, each amide unit forms both a $\text{Na-N}(\text{pyridyl})\text{-Na}$ and $\text{Na-N}(\text{amido})\text{-Na}$ bridge. In contrast replacing the phenyl ring with a second pyridyl ring in **2** results in loss of the $\text{N}(\text{pyridyl})$ bridge in exchange for two dative $\text{Na-N}(\text{pyridyl})$ interactions with a terminally attached, *syn-syn* dpa ligand (Fig. 3). Related studies by Liddle and Clegg have established a series of alkali metal complexes based upon the related parent amines 2-phenylaminopyridine^{33–35} and 2-trimethylsilylaminopyridine,^{36,37} including the crown ether solvates $[\{\text{Na}(\text{12C4})_2^+\}(\text{L}^-)]$ and $[\{\text{K}(\text{L})(\text{12C4})_2\}]^{38}$.

As would be anticipated according to the close similarity between isoelectronic PMDETA and TMDAE, sodium amide **3** exhibits a dimeric arrangement (Fig. 4) akin to that of **2**. The structure of **3** contains two crystallographically distinct Na centres, each of which engages in a didentate fashion with chelating TMDAE. Each hexa-coordinated Na also interacts with two bridging dpa units, both in a bidentate fashion, although the coordination mode differs. The first dpa ligand

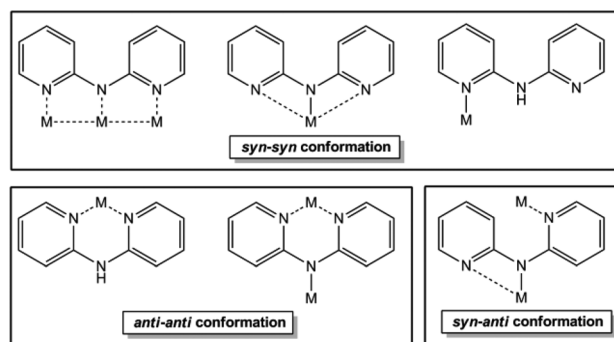


Fig. 3 Potential ligating modes of dpa(H) and dpa[−] towards a metal centre "M", displaying either *syn* [N(pyridyl) is directed the same way as N(amido)] or *anti* [N(pyridyl) is directed towards the neighbouring pyridyl ring] bonding conformations.

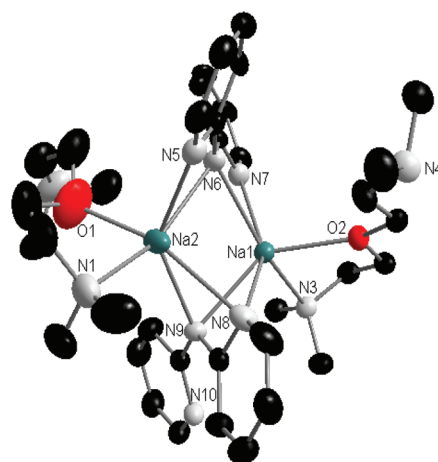


Fig. 4 Molecular structure of **3** with thermal ellipsoids at 50% probability level. Hydrogen atoms and minor disordered components of TMDAE have been omitted for clarity.

adopts a *syn-syn* conformation equivalent to that observed in **2**, where $\text{N}(\text{amido})$ bridges between two Na centres with two terminal $\text{N}(\text{pyridyl})\text{-Na}$ interactions providing further stabilisation. In contrast, the second dpa ligand occupies a *syn-anti* conformation, with $\text{N}(\text{amido})$ and $\text{N}(\text{syn-pyridyl})$ forming an unsymmetrical bridge [where the bridging Na1-N8 , Na1-N9 , Na2-N8 and Na2-N9 bond lengths are 2.680(4), 2.538(3), 2.752(4) and 2.496(3) Å, respectively]. As a result, **3** contains two central four-membered $[\text{NaNNa}]\text{N}$ rings at its core, each deviating from planarity with torsion angles of 15.281(2)° (Na2-N6-Na1-N9), and 35.359(2)° (Na1-N6-Na2-N8). Indicative of a small degree of resonance delocalisation within the dpa units, the dihedral angles between the pyridyl ring planes are relatively large [48.216° between the N5 and N7 pyridyl ring planes; 27.787° between the N8 and N10 pyridyl ring planes].

The chemistry of the tridentate, mixed N and O donor TMDAE is underdeveloped in comparison to that of its triamine counterpart, PMDETA. In this regard, **3** represents a rare example of a structurally characterised compound containing a non-substituted TMDAE donor. A search of the

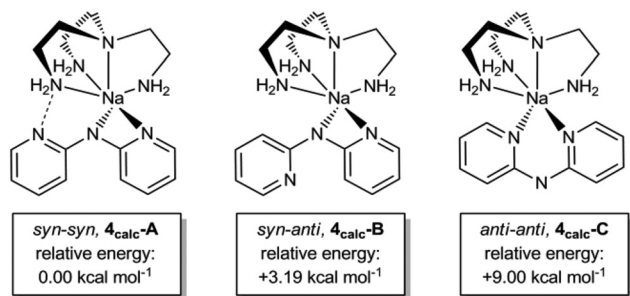


Fig. 5 Relative energies of DFT-models $4_{\text{calc-A-C}}$, representative of the regioisomers of complex **4**.

CSD³¹ surprisingly revealed that only one other compound involving a non-substituted TMDAE ligand has been structurally characterised, namely the solvated copper salt [(TMDAE)-CuCl₂].³⁹ In this example, TMDAE binds to Cu in a tridentate fashion. Illustrating the capability of TMDAE to act alternatively as a bidentate donor, the lithium aluminate [Li-(μ-Me₂NCH₂CH₂OCHCH₂NMe₂)(μ-TMP)Al(ⁱBu)₂] has also been structurally characterised,¹³ although in this case, TMDAE is an anion as it has also been subjected to deprotonation on a CH₂ unit adjacent to the O atom.

Unfortunately, repeated attempts to grow crystals of **4** suitable for X-ray diffraction analysis were unsuccessful as all were found to be badly disordered. We therefore turned again to a DFT study using the B3LYP method⁴⁰ and the 6-311G(d,p) basis set⁴¹ to facilitate the modelling of the molecular structure of **4**. Computations were performed to probe the relative energies of the conformational isomers of **4**, where dpa adopts either a *syn-syn* (model $4_{\text{calc-A}}$), *syn-anti* (model $4_{\text{calc-B}}$) or *anti-anti* (model $4_{\text{calc-C}}$) arrangement (Fig. 5). As H₆-TREN commonly acts as a monomerisation agent, $4_{\text{calc-A-C}}$ were modelled as monomeric species.^{42–46} Significantly, comparison of these model isomers revealed only a small difference in the relative energies of the three conformers, spanning just 9.00 kcal mol^{−1}. This closeness in the relative energy terms could be a factor in the severe disorder observed in the structure of crystalline **4**. Although model $4_{\text{calc-A}}$ is the energy minimum structure, the difference between $4_{\text{calc-A}}$ and $4_{\text{calc-B}}$ is very low at only 3.19 kcal mol^{−1}. However, for brevity, only the bond parameters of the thermodynamically favourable model $4_{\text{calc-A}}$ shall be discussed herein (Fig. 6).

Within $4_{\text{calc-A}}$, sodium engages *syn-syn* dpa in an asymmetric fashion (Na1–N1, 2.388 Å; Na1–N3, 2.539 Å, Na1...N2, 3.720 Å) and additional chelation by tetradentate H₆-TREN completes the highly congested, distorted octahedral coordination sphere [N–Na–N bond angles range from 55.1° to 159.2°]. Indicative of resonance delocalisation within the dpa scaffold, the C–(amido)N bond lengths of dpa are short [1.351 and 1.353 in $4_{\text{calc-A}}$ cf. 1.362 and 1.363 Å in 2_{calc}]. Furthermore, the bond lengths are indicative of a N–C=C–C=C–C–N pyridyl pattern (bond lengths 1.334/1.333, 1.389/1.389, 1.399/1.400, 1.381/1.380, 1.427/1.428, 1.368/1.373 Å), although the different N and H substituents give rise to a significant difference

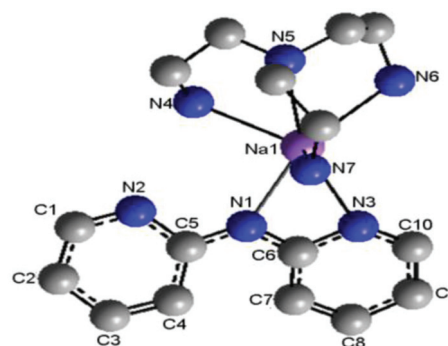


Fig. 6 DFT model of $4_{\text{calc-A}}$ with hydrogen atoms omitted for clarity. Selected bond lengths (Å) and bond angles (°): Na1–N1, 2.388; Na1...N2, 3.720; Na1–N3, 2.539; Na1–N4, 2.516; Na1–N5, 2.756; Na1–N6, 2.526; Na1–N7, 2.510; N1–C5, 1.353; N1–C6, 1.351; N2–C1, 1.334; N2–C5, 1.368; N3–C6, 1.373; N3–C10, 1.333; C1–C2, 1.389; C2–C3, 1.399; C3–C4, 1.381; C4–C5, 1.427; C6–C7, 1.428; C7–C8, 1.380; C8–C9, 1.400; C9–C10, 1.389; N1–Na1–N3, 55.1; N1–Na1–N4, 86.3; N1–Na1–N5, 138.8; N1–Na1–N6, 151.6; N1–Na1–N7, 91.9; N3–Na1–N4, 131.1; N3–Na1–N5, 159.2; N3–Na1–N6, 99.1; N3–Na1–N7, 99.5; N4–Na1–N5, 69.7; N4–Na1–N6, 107.2; N4–Na1–N7, 111.8; N5–Na1–N6, 69.5; N5–Na1–N7, 68.4; N6–Na1–N7, 105.3.

between the 'C–C' bonds. With steric congestion about the Na centre blocking a second Na–N(pyr) dative interaction, the non-coordinated pyridyl N2 is stabilised through the formation of a hydrogen bond with H₆-TREN [N2...H(N4), 2.068 Å, N2...N4, 3.071 Å]. A similar delocalisation of the anionic charge has been observed in alkali metal complexes bearing the related 2-phenylamidopyridine anion.³⁸

Although the application of either H₆- or Me₆-TREN as a highly chelating Lewis donor has been studied extensively within the context of transition metal chemistry, similar studies within s-block chemistry are less well evolved. Nonetheless, more recently structural studies of alkali metal-TREN complexes have been forthcoming. A representative selection is shown in Fig. 7, including 13 monomeric examples.^{42–46} For example, the amido lithium anionic crown [{Me₆-TREN}Li-(μ-Cl)Li{Me₆-TREN}]⁺[Li₅(μ-HMDS)₅Cl][−], provides a cationic example (Fig. 7c), with a linear Li–Cl–Li unit at its core.⁴⁵ Another unusual example is the tetranuclear lithium compound [Li₂(OAr^{Me})₂·Me₆TREN]₂, which demonstrates the good bridging ability of OAr^{Me} ligands.⁴³

Solution state characterisation of sodium amides 2–4

Multinuclear (¹H, ¹³C{¹H}) NMR spectroscopic analysis of sodium amide complexes **2–4** in *d*₈-THF solution confirmed that in each case, mono-deprotonation of dpa(H) has occurred with the loss of the N–H resonance at 8.83 ppm. As a consequence of dpa(H) metallation, the four aromatic resonances (labelled H1–H4) experience a significant low frequency shift (Table S2†). For example, the H4-dpa resonance deviates upfield from 7.72 ppm in the parent amine dpa(H), by 0.65 ppm in **2**, 0.42 ppm in **3** and 0.57 ppm in **4**. On the basis of this information it appears that aggregation (in **2** and **3**) has less bearing on these chemical shifts than the local coordi-

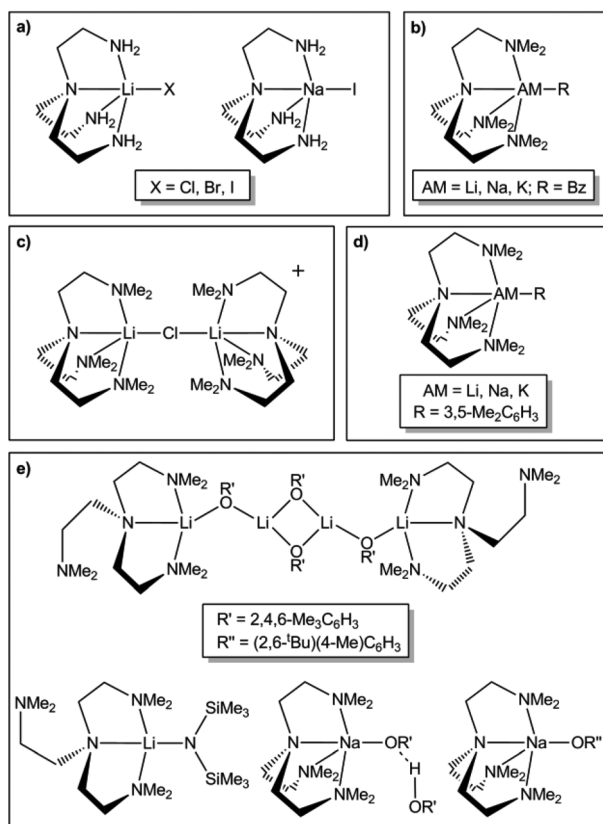


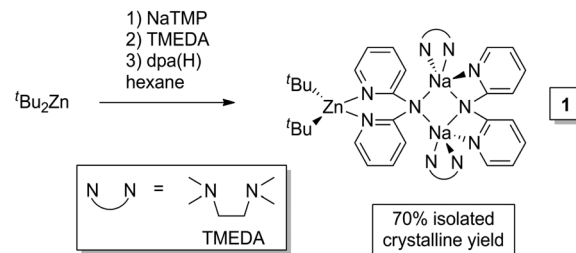
Fig. 7 Graphical representation of the molecular structures of s-block-TREN complexes (a) ref. 42, (b) ref. 44, (c) ref. 45, (d) ref. 46, (e) ref. 43.

nation environment of the Na centre. Within the $^{13}\text{C}\{\text{H}\}$ NMR spectra, metallation of dpa(H) translates as a downfield shift of the C_{ipso} resonance, by 11.4 ppm in 2, 7.4 ppm in 3 and 11.2 ppm in 4.

Comparison of the ^1H NMR spectroscopic resonances attributed to PMDETA in 2 with those of non-coordinated PMDETA give good agreement in d_8 -THF solvent [NCH_2 , 2.42 and 2.31 ppm; NCH_3 , 2.18 ppm; $\text{N}(\text{CH}_3)_2$, 2.14 ppm]. Thus, the bulk Lewis donor solvent d_8 -THF is exposed as a non-innocent solvent medium, which displaces the trifunctional amine from coordination to the electropositive Na centre in solution. Moreover, this finding is mirrored by the resonances ascribed to TMDAE and H_6 -TREN within 3 and 4 respectively, which are in close agreement with those of non-coordinated TMDAE and H_6 -TREN in d_8 -THF solution.

Evaluating formation of a bimetallic sodium–zinc product upon co-complexation of $^t\text{Bu}_2\text{Zn}$ with sodium amides 2, 3 and 4

Evidence that combining metalloligand $[(\text{TMEDA})\text{Na}(\text{dpa})]_2$ with $^t\text{Bu}_2\text{Zn}$ results in the formation of a co-complex comes in the form of the previously reported donor–acceptor sodium–zinc compound $\{[(\text{TMEDA})\text{Na}(\text{dpa})]_2\text{Zn}^t\text{Bu}_2\}$ (**1**) (Scheme 2).²⁴ Attempts to ascertain whether 2, 3 and 4 can also behave as metalloligands towards $^t\text{Bu}_2\text{Zn}$ were carried out through the 2 : 1 equimolar combination of sodium amides $[(\text{PMDETA})\text{Na}$



Scheme 2 Synthesis of sodium zincate $\{[(\text{TMEDA})\text{Na}(\text{dpa})]_2\text{Zn}^t\text{Bu}_2\}$ (**1**).²⁴

(dpa)], $[(\text{TMDAE})\text{Na}(\text{dpa})]$ or $[(\text{H}_6\text{-TREN})\text{Na}(\text{dpa})]$ with $^t\text{Bu}_2\text{Zn}$, whereupon each reaction mixture was studied *via* ^1H NMR spectroscopy in C_6D_6 solution (Table S3†). Unfortunately, repeated attempts to grow crystals of these putative co-complexes suitable for X-ray diffraction analysis were unsuccessful. That notwithstanding, detection of resonances attributed to $[(\text{donor})\text{Na}(\text{dpa})]$ (where donor is PMDETA, TMDAE or H_6 -TREN) and $^t\text{Bu}_2\text{Zn}$ in a 2 : 1 ratio, infers the formation of a sodium–zinc co-complex. Since non-coordinated $^t\text{Bu}_2\text{Zn}$ is highly volatile under reduced pressure at ambient temperature, it would have been removed *in vacuo* on preparing the samples. Examination of the $^t\text{Bu}_2\text{Zn}$ resonances, which are different in each case (1.58 ppm in 2; 1.53 ppm in 3, 1.66 ppm in 4) confirms there is a considerable shift towards higher frequency in comparison to non-coordinated $^t\text{Bu}_2\text{Zn}$ (1.08 ppm in C_6D_6 solution). Incorporation of $^t\text{Bu}_2\text{Zn}$ also significantly alters the resonances associated with the sodium amide moieties 2–4 (Table S3†). For example, upon addition of $^t\text{Bu}_2\text{Zn}$ to 2, H3-dpa experiences an upfield shift of 0.16 ppm, whilst the PMDETA- $\text{N}(\text{CH}_3)_2$ resonance moves upfield by 0.19 ppm.

Diffusion ordered spectroscopy (DOSY) experiments in C_6D_6 solution on sodium amides 2–4 in the presence of $^t\text{Bu}_2\text{Zn}$ suggest that all of these amides are co-complexed with the zinc reagent but that their respective donor ligands, PMDETA, TMDAE, and H_6 -TREN compete with C_6D_6 solution molecules in coordinating to the sodium (see ESI† for full details).

Although di-*tert*-butylzinc free **2_{calc}** and di-*tert*-butylzinc containing **1** have different Lewis donor components, the didentate coordination mode of trifunctional PMDETA within **2_{calc}** mimics that of difunctional TMEDA within **1**. Thus the similarity between the sodium amide component of **2_{calc}** and **1** allows for tentative comparisons to be drawn. Within **2_{calc}**, the steric congestion at Na is reflected by the narrow N–Na–N bite angle of 67.8° for PMDETA, which is considerably smaller than the corresponding TMEDA bite angles within **1** [N–Na–N bond angles are $74.63(5)^\circ$ and $74.18(6)^\circ$]. It therefore seems logical that in **1**, coordination of the metalloligand $\{[(\text{TMEDA})\text{Na}(\text{dpa})]_2\}$ towards $^t\text{Bu}_2\text{Zn}$ relieves the steric strain at the Na centre, as one dpa unit welcomes $^t\text{Bu}_2\text{Zn}$ into its pyridyl pocket by switching its coordination mode from *syn-syn* to *anti-anti*. Investigation into the dpa bond lengths of the sodium precursor **2_{calc}** suggests that the anionic charge of

each dpa ligand is coupled into the pyridyl rings through resonance delocalisation. This contrasts with the pattern observed in **1**, where although the anionic charge is delocalised throughout the *syn-syn* dpa unit, the anionic charge of the *anti-anti* dpa unit is predominantly focussed on N(amido). It seems plausible that this difference is due to the steric requirements of tetrahedrally coordinated Zn interrupting the planar geometry usually observed with resonance delocalisation. Structural modelling of the $\{(\text{TMEDA})\text{Na}(\text{dpa})\}_2$ metallo-ligand, **8_{calc}**, through DFT calculations revealed close similarities between **2_{calc}** and **8_{calc}** (refer to ESI† for further detail). The gross structural factors remain the same: Na adopts a distorted octahedral coordination sphere and both dpa ligands adopt a *syn-syn* conformation with the anionic charge coupled into the pyridyl rings.

Reactivity studies: investigating the outcome of varying the Lewis donor upon benzophenone alkylation

It has long been known that the addition of Lewis donors to polar organometallic reagents can significantly alter their structures^{47–50} leading to changes in their reactivity.⁵¹ In the case of organoalkali metal compounds this change can normally be an enhancement due to deaggregation effects; whereas with organoaluminium compounds it can have a

detrimental effect on the reaction because reactive three coordinate monomers can be transformed into inert four coordinate species. We therefore decided to investigate the effect of modifying the Lewis donor within our metalloligand system (Table 1). A range of donors was investigated, including the mixed O/N donors TEMPO (2,2,6,6-tetramethylpiperidine-*N*-oxyl radical) and TMDAE, and the all N donors DMAP (4-dimethylaminopyridine), TMEDA, PMDETA, H₆-TREN and Me₆-TREN.

Using the homometallic zinc reagent ^tBu₂Zn without a supporting sodium amide, a miserable 1% yield of the 1,6-(*para*)-addition product was obtained at ambient temperature, with no other addition products detected, but only unreacted benzophenone. However, introduction of the sodium dipyridyl-amide metallo-ligand with DMAP, TMEDA or PMDETA as the Lewis donor boosted the reactivity of ^tBu₂Zn, leading to moderate *para*-alkylation yields of 24% (entry 2), 40% (entry 4) and 43% (entry 5), respectively. In each case, *para*-addition was obtained as the major product hinting at a common mechanism within these donor distinct reactions. In contrast, using TEMPO, TMDAE, H₆-TREN or Me₆-TREN as the Lewis donor gave no significant reactivity enhancement over ^tBu₂Zn (entries 3 and 6–8). It is noteworthy that using the TMDAE metallo-ligand under reflux conditions led to a sizeable improvement

Table 1 Reaction of zinc reagents with benzophenone in hexane solvent

$ \begin{array}{c} \text{1) } ^t\text{Bu}_2\text{Zn (1 equiv.)} \\ \text{[(donor)Na(dpa)] (2 equiv.)} \\ \text{hexane} \\ \text{2) H}_2\text{O, O}_2 \end{array} \rightarrow \begin{array}{c} \text{Ph-C(=O)-Ph} \\ \\ \text{Ph} \end{array} + \begin{array}{c} \text{OH} \\ \\ \text{Ph-CH-Ph} \\ \\ ^t\text{Bu} \end{array} + \begin{array}{c} \text{OH} \\ \\ \text{Ph-C(=O)-Ph} \\ \\ ^t\text{Bu} \end{array} + \begin{array}{c} \text{OH} \\ \\ \text{Ph-CH-Ph} \\ \\ \text{H} \end{array} $						
Product yield ^a (%)						
Entry	Donor	Reaction temp. (°C)	<i>para</i> -Addition (1, 6-)	Carbonyl-addition (1, 2-)	<i>ortho</i> -Addition (1, 4-)	Benzhydrol (H ⁺ addition) Total
Stoichiometric conditions^b						
1	None ^{c, 24}	r.t.	1	0	0	0
2	DMAP	r.t.	24	6	0	5
3	TEMPO	r.t.	0	0	0	1
4	TMEDA ²⁴	r.t.	40	6	1	8
5	PMDETA	r.t.	43	2	1	11
6	TMDAE	r.t.	2	1	0	0
7	H ₆ -TREN	r.t.	2	1	0	4
8	Me ₆ -TREN	r.t.	1	1	0	1
9	None ^{c, 24}	75	11	1	0	8
10	DMAP	75	25	14	0	8
11	TMEDA ²⁴	75	44	11	2	14
12	PMDETA	75	46	3	1	10
13	TMDAE	75	45	9	1	3
14	H ₆ -TREN	75	5	4	0	7
15	Me ₆ -TREN ^d	75	34	13	0	11
Sub-stoichiometric conditions^e						
16	DMAP	75	26	8	0	7
17	TMEDA ²⁴	75	52	12	0	7
18	PMDETA	75	53	6	0	6
19	TMDAE	75	25	7	0	3

^a Yields determined by ¹H NMR spectroscopy using hexamethylbenzene (10 mol%) as an internal standard. ^b Conditions: Nadpa (2 mmol), donor (2 mmol), ^tBu₂Zn (1 mmol), PhC(=O)Ph (1 mmol), hexane (8 mL) for 18 hours. ^c ^tBu₂Zn alone was used as the reagent. ^d The reaction was performed four times and the yields proved variable, with the 1,6-addition product ranging from 26% to 41% (refer to ESI for further details).

^e Conditions: Nadpa (1 mmol), donor (1 mmol), ^tBu₂Zn (5 mmol), PhC(=O)Ph (5 mmol), hexane (40 mL) for 18 hours.

of the *para*-alkylation yield, from 2% to 45% at 75 °C (compare entries 6 and 13). This surprising result was mirrored by Me₆-TREN, as moving to reflux conditions increased the *para*-alkylation yield to 34% (entries 8 and 15). As aforementioned, using sub-stoichiometric quantities (10 mol%) of **1** gives a 52% yield of the *para*-addition product.²⁴ This enhanced ^tBu₂Zn reactivity is successfully reflected when using sub-stoichiometric quantities of PMDETA-containing metalloligand **2**, culminating in a 53% yield of *para*-addition (entry 18) and suggesting that the metalloligand can be recycled to a modest degree within this reaction system. Again the clear preference for *para*-addition in nearly all of these reactions suggests a similar mechanism though the activation barriers appear to be higher for TMDAE and Me₆-TREN as they require higher temperature to achieve greater *para*-addition.

Selection of PMDETA as the Lewis donor gives competitive *para*-addition yields to those obtained using TMEDA (respective yields of 43% and 40% at ambient temperature, entries 4 and 5). The fact that in the molecular structure of **2**, PMDETA mimicks TMEDA by acting as a didentate donor towards sodium, seems likely to have a bearing on these similar results. It seems unlikely that this asymmetric bonding mode is retained in C₆D₆ solution, as spectroscopic analysis of **2** in this aromatic hydrocarbon medium reveals only one set of resonances corresponding to PMDETA. Alternatively, the triamine could be undergoing a fast exchange process. Furthermore, DOSY analysis of **2** with ^tBu₂Zn in C₆D₆ solvent suggests that C₆D₆, which can act as a Lewis donor, is in competitive equilibrium with PMDETA. However, as **2** is crystallised from the non-polar solvent hexane, it seems plausible that the hexane solution state structure of **2** mirrors that of the solid state structure.

Despite their close similarity, exchanging PMDETA for iso-electronic TMDAE markedly reduces the yield of the *para*-product (most noticeably from 43% to 2% at ambient temperature, entries 5 and 6). As could be expected based on the likeness of PMDETA and TMDAE, precursor complexes **2** and **3** adopt similar solid state structures: both are dimeric, each potentially tridentate Lewis donor bonds to sodium in a didentate fashion, and the two Na centres of each dimer are bridged *via* the amido N of deprotonated dpa. However, there are two

key distinctions between **2** and **3**. The donor chelation in **2** is *via* two N atoms, whereas in **3** it is *via* one O and one N atom. Also, within **2**, both dpa units adopt a *syn-syn* conformation, whilst in contrast the two dpa units within **3** differ in their conformation. The first mirrors the *syn-syn* bonding observed within **2**, whilst the second adopts a *syn-anti* conformation, connecting the two Na centres *via* two Na–N(amido) and two Na–N(*syn*-pyridyl) interactions.

Functioning as a protective ligand shield to partly cover an alkali metal cation (Fig. 7), tetradentate H₆-TREN and Me₆-TREN have the capacity to act as monomerisation agents toward organometallic species including alkali metal benzyl⁴⁴ and 3,5-dimethylbenzyl⁴⁶ salts, where the alkali metal is lithium, sodium or potassium. This ability is again reflected in the molecular structure of crystalline **4** (refer to ESI†). The detrimental effect of H₆-TREN (and Me₆-TREN) upon reactivity could therefore be an artefact of too much steric shielding of the Na centre. As aforementioned, the solution NMR data point to a co-complex between Nadpa and ^tBu₂Zn with possibly the TREN ligands going on and off the sodium atoms so the steric shielding could be manifested in monomeric structures in contrast to the dimeric structures seen with the other donors. These findings show that careful selection of the donor ligand is crucial to ensure that the reaction yields are not compromised.

Evaluating the reaction dependency of the alkali metal

As the best *para*-alkylation yields were obtained using PMDETA as the donor, this system was chosen to probe the effect of changing the alkali metal component of the metalloligand. Remarkably, simply substituting Na by Li destroyed the regioselectivity of the reaction, giving a mixture of *para*- and carbonyl-addition and benzhydrol in a relative ratio of approximately 1 : 1 : 1 (Table 2, entry 1). Surprisingly, the reaction was almost completely suppressed when K was employed as the alkali metal, with an insignificant 2% yield of *para* product obtained (Table 2, entry 3) along with unreacted benzophenone. Thus the size and Lewis acidity of the alkali metal significantly impacts upon the yield and regioselectivity of the reaction, with the optimum results obtained using the intermediately sized Na. These findings bear some comparison to

Table 2 Reactions of alkali metal dipyriddyamide, PMDETA, ^tBu₂Zn and benzophenone in hexane solvent for 18 hours at ambient temperature

$\text{PhC(=O)Ph} \xrightarrow[\text{hexane}]{\begin{matrix} 1) \text{ } ^t\text{Bu}_2\text{Zn (1 equiv.)} \\ [(\text{PMDETA})\text{M(dpa)}] \text{ (2 equiv.)} \\ 2) \text{ H}_2\text{O, O}_2 \end{matrix}} \text{PhC(=O)C}_6\text{H}_4\text{C(=O)Ph} + \text{PhC(=O)C}_6\text{H}_4\text{OH} + \text{PhC(=O)C}_6\text{H}_3\text{(OMe)}_2 + \text{PhC(=O)C}_6\text{H}_4\text{OH} + \text{PhC(=O)C}_6\text{H}_4\text{OH}$						
Product yield ^{a,b} (%)						
Entry	Metal M	<i>para</i> -Addition (1, 6-)	Carbonyl-addition (1, 2-)	<i>ortho</i> -Addition (1, 4-)	Benzhydrol (H ⁺ addition)	Total
1	Li	21	19	0	18	58
2	Na	43	2	1	11	57
3	K	2	2	0	0	4

^a Yields determined by ¹H NMR spectroscopy using hexamethylbenzene (10 mol%) as an internal standard. ^b Conditions: Mdp (2 mmol, M = Li, Na or K), PMDETA (2 mmol), ^tBu₂Zn (1 mmol), PhC(=O)Ph (1 mmol), hexane (8 mL) for 18 hours at ambient temperature.

Table 3 Reaction of zincate $[(\text{TMEDA})\text{Na}(\text{dpa})]_2\text{Zn}^t\text{Bu}_2$ (**1**) with benzophenone for 18 hours at ambient temperature

$\text{Ph-C(=O)-Ph} \xrightarrow[\text{2) } ^t\text{H}_2\text{O, O}_2]{\text{1) } ^t\text{Bu}_2\text{Zn (1 equiv.)} \atop [(\text{TMEDA})\text{Na}(\text{dpa})] \text{ (2 equiv.)} \atop \text{solvent}} \text{Ph-C(=O)-Ph} + \text{Ph-C(OH)(}^t\text{Bu)-Ph} + \text{Ph-C(=O)-}^t\text{Bu} + \text{Ph-C(OH)(H)-Ph}$						
Entry	Solvent	Product yield ^{a,b} (%)				Total
		<i>para</i> -Addition (1, 6-)	Carbonyl-addition (1, 2-)	<i>ortho</i> -Addition (1, 4-)	Benzhydrol (H^- addition)	
1	Hexane	40	6	1	8	55
2	Hexane-THF ^c	7	3	0	1	11
3	THF	11	3	0	1	15

^a Yields determined by ^1H NMR spectroscopy using hexamethylbenzene (10 mol%) as an internal standard. ^b Conditions: Nadpa (2 mmol), TMEDA (2 mmol), $^t\text{Bu}_2\text{Zn}$ (1 mmol), PhC(=O)Ph (1 mmol), solvent (8 mL) for 18 hours at ambient temperature. ^c A 1 : 1 ratio of hexane-THF solvent was used.

previous studies by Ishihara, where moving from the organolithium reagent $^n\text{BuLi}$, to the related Grignard reagent $^n\text{BuMgCl}$, changed the major product from that of carbonyl-addition (in a 58% yield) to benzhydrol (in a 56% yield), but significantly no *para*-addition was evident in either case.²²

Exploring the reaction dependency of the solvent

Curious to find out whether or not increasing the solvent polarity would improve the reaction yield, we next investigated Lewis basic THF as the bulk solvent in the reaction of **1** with benzophenone. However, a significant diminution of the *para*-addition yield was observed, from 40% in hexane solvent to 11% in neat THF solution (Table 3, respective entries 1 and 3). Analysis of crystalline **1** in C_6D_6 solvent suggests that TMEDA coordinates to Na in this medium, as a significant upfield shift is observed for the CH_2 -TMEDA and CH_3 -TMEDA resonances (by 0.66 and 0.38 ppm respectively from their values in free TMEDA, Table S4, entries 1 and 2 \ddagger). In contrast, when lone pair coordinating d_8 -THF was used as the solvent, the TMEDA resonances attributed to TMEDA within **1** give close agreement with those of non-coordinated TMEDA (Table S4, entries 3 and 4 \ddagger).

It has long been recognised in organoalkali metal chemistry that the solution state structure does not always reflect the solid state structure as the former is often more complicated involving multiple species and dynamic processes.^{1,52–56} Far from being an idle spectator, d_8 -THF participates through the displacement of TMEDA within **1**, which is accompanied by low reaction yields. It therefore seems logical that the microscopic coordination at the sodium centre is key, and that the coordination of stoichiometric TMEDA in comparison to the effect of using bulk THF plays a pivotal role in the extent and selectivity of the alkylation reaction. Indeed, it could in fact be the decoordination of TMEDA, which is paramount to the success of the nucleophilic addition, through creating a vacant site at the Lewis acidic sodium centre. It follows that this could facilitate the coordination of the Lewis donor benzophenone towards sodium, hence bringing it into close proximity with the activated $^t\text{Bu}_2\text{Zn}$ fragment.

^1H NMR spectroscopic analysis of **1** in d_8 -THF solution exhibits a resonance attributed to the ^tBu groups at 0.87 ppm, an upfield deviation of just 0.11 ppm in comparison to free $^t\text{Bu}_2\text{Zn}$ (at 0.98 ppm in d_8 -THF solution). Upon moving to C_6D_6 solvent, a more significant difference of 0.49 ppm is observed, where this time the ^tBu resonance of **1** (at 1.57 ppm) lies further downfield than that of free $^t\text{Bu}_2\text{Zn}$ (at 1.08 ppm). It therefore seems plausible that bulk THF solvent extrudes, or mostly extrudes $^t\text{Bu}_2\text{Zn}$ from the $[(\text{TMEDA})\text{Na}(\text{dpa})]_2\text{Zn}^t\text{Bu}_2$ co-complex; whereas in C_6D_6 solvent it remains fully attached.

The effect of substituting $^t\text{Bu}_2\text{Zn}$ by $^t\text{BuLi}$ as the *tert*-butyl source was also evaluated. It was found that substituting $^t\text{Bu}_2\text{Zn}$ by $^t\text{BuLi}$ as the *tert*-butyl ligand source in combination with $[(\text{PMDTA})\text{Na}(\text{dpa})]$ shuts down any *para*-addition, with the yield falling from 48% to 0% (see ESI \ddagger for full details).

Turning from tertiary alkyl ^tBu to primary alkyl CH_2SiMe_3

Previous studies of the alkylation of benzophenone using polar organometallic reagents have shown the product distribution to be dependent on the nature of the alkyl group.⁵⁷ For example, the reaction of $^n\text{PrMgBr}$ with a range of *para*-substituted benzophenone substrates gave only carbonyl-addition and benzhydrol products; whereas *ortho*-addition was also observed using the branched isomer, $^i\text{PrMgBr}$. Intrigued by these findings, we decided to investigate R_2Zn as an alkyl transfer reagent (where R is CH_2SiMe_3). On account of the stabilising α -silyl group upon the trimethylsilylmethyl “carbanions”, R_2Zn behaves as a more gentle reagent than $^t\text{Bu}_2\text{Zn}$ when combined with a sodium amide in a molecular environment.⁵⁸

In this experiment, freshly prepared R_2Zn was added to metalloligand $[(\text{TMEDA})\text{Na}(\text{dpa})]_2$ in a 1 : 1 ratio in hexane solvent. Multinuclear (^1H , $^{13}\text{C}\{\text{H}\}$) NMR spectroscopic analysis of the resultant white solid dissolved in C_6D_6 solvent revealed resonances attributable to dpa, TMEDA and R_2Zn . Although the solubility of this white solid in C_6D_6 solvent is limited, its ^1H NMR spectrum shows a 2 : 2 : 1 ratio of dpa-TMEDA- R_2Zn resonances, which hints that the soluble product is contaminated with a second, insoluble product still visible in the NMR sample (*vide infra*). These resonances mostly deviate upfield

Table 4 Comparison of ^1H NMR data (C_6D_6 , 400.03 MHz, 300 K) for TMEDA, R_2Zn , dpa(H) and **5** ($\text{R} = \text{CH}_2\text{SiMe}_3$)

Atom assignment	Chemical shift (ppm)			
	TMEDA	R_2Zn	dpa(H)	5
TMEDA (NCH_3)	2.12	—	—	1.86
TMEDA (NCH_2)	2.35	—	—	1.82
$\text{R} [\text{CH}_2\text{Si}(\text{CH}_3)_3]$	—	−0.62	—	−1.02
$\text{R} [\text{CH}_2\text{Si}(\text{CH}_3)_3]$	—	0.08	—	0.39
dpa (H1)	—	—	8.16	8.01
dpa (H2)	—	—	6.75	6.27
dpa (H3)	—	—	7.53	7.10
dpa (H4)	—	—	7.72	7.10

from those of the parent amine dpa(H), non-coordinated TMEDA and non-coordinated R_2Zn (Table 4). For example, the respective $\text{ZnCH}_2\text{Si}(\text{Me})_3$ and $\text{ZnCH}_2\text{Si}(\text{CH}_3)_3$ resonances shift by 0.40 ppm upfield and 0.31 ppm downfield when combined with the metalloligand $[(\text{TMEDA})\text{Na}(\text{dpa})]_2$. This suggests that a co-complex of empirical formula $[(\text{TMEDA})\text{Na}(\text{dpa})]_2\text{ZnR}_2$ (**5**) is formed, indicating that it belongs to the same family as **1**. However, this system departs from **1**, as **1** is fully soluble in C_6D_6 solvent and thus no insoluble by-products are observed.

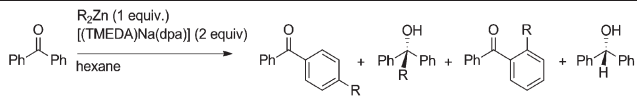
Upon the ambient temperature reaction of **5** with benzophenone in hexane, only a trace (<1%) of the *para*-addition product was observed, providing a marked reduction from the 40% yield of *para*-addition obtained using the *tert*-butyl variant **1** under identical reaction conditions (Table 5, entries 1 and 2). Using **5** under reflux conditions did not improve the yields of *para*-⁵⁹ and carbonyl-alkylation,⁶⁰ although a low yield of benzhydrol was obtained (8%, Table 5, entry 3). Previous studies have suggested that the alkylation of benzophenone occurs through a single electron transfer (SET) reaction mechanism,⁵⁷ and the product distribution has therefore been linked to radical stability. If this alkylation reaction were to proceed through a SET pathway, the lesser stability of the primary R radical in comparison to the tertiary ^tBu radical

is likely to be a key factor towards the significantly diminished alkylation yields.⁶¹

Evaluating the effect of adding TEMPO to the reaction system

Described recently as a “chameleonic ligand” due to its different forms,^{62,63} the nitroxide TEMPO can perform as a Lewis base either in its native radical form, or its reduced, anionic form (TEMPO[−]). Often exploited as a radical trapping reagent,⁶⁴ TEMPO can also be used to provide insight into a postulated reaction mechanism.⁶⁵ For instance, $[(\text{TMEDA})\text{Na}(\mu\text{-TMP})(\mu\text{-}^t\text{Bu})\text{Zn}^t\text{Bu}]$, which can regioselectively *tert*-butylate benzophenone at the *para*-position,⁸ undergoes a redox reaction with TEMPO to afford the crystalline triheteroleptic sodium zincate $[(\text{TMEDA})\text{Na}(\mu\text{-TMP})(\mu\text{-TEMPO}^*)\text{Zn}^t\text{Bu}]$. In this example, TEMPO has been reduced to its anion TEMPO[−] with concomitant formation of a ^tBu radical, which is thought to react with another ^tBu radical to produce iso-butane and iso-butene. Thus this study provides evidence that $[(\text{TMEDA})\text{Na}(\mu\text{-TMP})(\mu\text{-}^t\text{Bu})\text{Zn}^t\text{Bu}]$, normally thought to be an anionic base source, can also combine through a SET mechanism.⁶⁵ To compare with these findings, we incorporated TEMPO into our alkylation system, to probe its effect upon the reaction outcome. It transpired that the addition of TEMPO to metallo-ligand $[(\text{PMDETA})\text{Na}(\text{dpa})]_2$, $^t\text{Bu}_2\text{Zn}$ and benzophenone completely destroyed the nucleophilic releasing ability of $[(\text{PMDETA})\text{Na}(\text{dpa})]_2\text{-}^t\text{Bu}_2\text{Zn}$. Accordingly, only an insignificant trace of the *para* product was observed (1% yield compared to 48% in the absence of TEMPO). Multinuclear (^1H , $^{13}\text{C}\{^1\text{H}\}$) NMR spectroscopic analysis of the crude reaction mixture confirmed that the known nitroxide compound TEMPO- ^tBu was present, alongside unreacted benzophenone.⁶⁶ Diagnostic of TEMPO- ^tBu , two distinctive singlets arising from the two inequivalent methyl groups of the nitroxide are observed at 1.15 and 1.10 ppm. A sharp singlet attributed to the ^tBu group is also seen at 1.28 ppm. Completing the assignment, multiplets corresponding to β -TEMPO and γ -TEMPO hydrogen atoms were observed at 1.48 and 1.30 ppm respectively in a ^1H NMR spectrum recorded in CDCl_3 solvent.

Table 5 Reaction of zinc reagents with benzophenone in hexane solvent for 18 hours

						
			Product yield ^{a,b} (%)			
Entry	R	Reaction temp. (°C)	<i>para</i> -Addition (1,6-)	Carbonyl- addition (1,2-)	Benzhydrol (H^- addition)	Total
1	CH_2SiMe_3	r.t.	0	0	0	0
2	$^t\text{Bu}^{24}$	r.t.	40	6	8	54
3	CH_2SiMe_3	75	0	0	8	8
4	$^t\text{Bu}^{24}$	75	33	11	14	58

^a Yields were determined by ^1H NMR spectroscopy using hexamethylbenzene (10 mol%) as an internal standard. ^b Conditions: Nadpa (2 mmol), TMEDA (2 mmol), R_2Zn , (1 mmol), PhC(=O)Ph (1 mmol), hexane (8 mL) for 18 hours at ambient temperature.

Mechanistic insights

The nature of the mechanism for the addition of polar organo-metallic reagents to ketones has posed a long standing question, where the two major contending mechanisms involve a single electron transfer (SET) reaction pathway, or a polar reaction mechanism. Evidence to support a SET pathway for the alkylation of benzophenone has been accrued,^{67,68} including the observation of the homo-coupled side-product benzopinacol [$\text{Ph}_2\text{C}(\text{OH})\text{C}(\text{OH})\text{Ph}_2$].⁶⁹ Furthermore, Ashby and Bowers observed the cyclisation of a radical probe incorporated into a Grignard reagent, which infers that an alkyl radical species was formed prior to addition to benzophenone.⁷⁰

The inhibition of our alkylation reaction by TEMPO, combined with the interception of a ^tBu radical in the formation of TEMPO- ^tBu , initially implied that this reaction could follow a SET reaction pathway. To gain further insight into the reaction system, TEMPO was added to a hexane solution of $^t\text{Bu}_2\text{Zn}$, upon which the characteristic red-orange colour associated with the TEMPO radical disappeared. Cooling the resultant colourless solution to -30°C afforded a crystalline solid after 24 hours. Unfortunately, severe disorder in the crystallographic structure made it impossible to refine the molecular structure satisfactorily; hence no structural data can be presented. However, NMR spectroscopic analysis of the crystalline material in C_6D_6 solution confirmed the presence of anionic TEMPO* in addition to *tert*-butyl ligands in a 1 : 1 ratio and so its formula therefore appears to be $[(\text{TEMPO}^*)\text{Zn}(^t\text{Bu})]$ (yield 0.08 g; 29%). Carmona has previously reported the structural characterisation of the related heteroleptic dimer, $[(\text{TEMPO}^*)\text{Zn}(\text{Et})_2]$.⁷¹ Present in the filtrate, TEMPO- ^tBu was also produced from the reaction of $^t\text{Bu}_2\text{Zn}$ with TEMPO, as evidenced through NMR spectroscopy.

Given the propensity of TEMPO to act as a Lewis base ligand towards a metal centre, it cannot be ruled out that TEMPO shuts down the alkylation reaction by sequestering Zn from the sodium zinc co-complex. Henceforth, $[(\text{PMDTA})\text{Na}(\text{dpa})_2]$, $^t\text{Bu}_2\text{Zn}$ and TEMPO were combined in a 1 : 1 : 1 stoichiometric ratio in hexane solvent and the reaction mixture was analysed by NMR spectroscopy, which revealed resonances corresponding to TEMPO- ^tBu .⁶⁶ This suggests that TEMPO breaks up the synergic, sodium metalloligand/*tert*-butylzinc partnership by extracting a butyl radical from the zinc centre, which could be a factor in the inhibition of the benzophenone alkylation reaction. As a control comparison, the failure of the neutral heteroleptic zinc complex $[(\text{TEMPO}^*)\text{Zn}(^t\text{Bu})]$ to *tert*-butylate benzophenone, at any position, was tested and confirmed. It is also possible that TEMPO sequesters the alkali metal from the metalloligand complex. Most TEMPO coordination chemistry has been studied with d block,^{71–76} p block^{77–80} and f block elements,⁸¹ however more recently, structural studies of s block element-TEMPO structures have been carried out,^{62,63,65} including the alkali metal complexes $(\text{THF})_2[\text{Li}(\text{TEMPO}^*)]_4$ and $[(\text{THF})\text{Na}(\text{TEMPO}^*)]_4$.⁶³ With the data accumulated thus far, it is therefore impossible to unequivocally state that our reaction follows a radical pathway.

Although TEMPO- ^tBu was detected in the reaction mixture, this could either be produced from the interception of a ^tBu radical prior to its reaction with benzophenone, or generated as a side product from reaction of TEMPO with $^t\text{Bu}_2\text{Zn}$.

Although the reaction mechanism (or mechanisms) appears convoluted and is not yet well understood, it is clear that the choice of ligand has a considerable impact upon the reaction yield. In spite of this, observation of *para*-addition as the major product in each reaction system indicates that there is a common mechanism within these reactions. Previously, $^t\text{Bu}_2\text{Zn}\cdot\text{TMEDA}$ and $^t\text{Bu}_2\text{Zn}\cdot(\text{pyridine})_2$ were shown to be inactive towards the alkylation of benzophenone using our reaction conditions, whilst the sodium zinc donor-acceptor complex $\{[(\text{TMEDA})\text{Na}(\text{dpa})]_2\text{Zn}^t\text{Bu}_2\}$ generates 40% of the *para*-addition product at ambient temperature.²⁴ In contrast, highly coordinating ligands such as $\text{H}_6\text{-TREN}$ have an adverse effect upon the reaction yield, which could be an artefact of too much steric shielding of the Na centre, or that monomeric complexes are inactive compared to dimeric complexes. Changing the bulk solvent medium from non-polar hexane to Lewis donor THF, which displaces the donor ligands TMEDA, PMDETA, TMDAE and $\text{H}_6\text{-TREN}$ in the solution state, leads to a significant decrease in the alkylation yields. Furthermore, spectroscopic evidence points towards the displacement of $^t\text{Bu}_2\text{Zn}$ from the $\{[(\text{TMEDA})\text{Na}(\text{dpa})]_2\}$ metalloligand in $d_8\text{-THF}$ solvent. Preservation of the synergic sodium-zinc donor-acceptor complex therefore appears to be a dominant factor in the reactivity enhancement of the attacked $^t\text{Bu}_2\text{Zn}$ moiety.

Conclusions

A synergic reactivity is clearly operative in these alkylation reactions. Co-complexation of sodium dipyriddyamide metalloligands $[(\text{TMEDA})\text{Na}(\text{dpa})_2]$, $[(\text{PMDETA})\text{Na}(\text{dpa})_2]$, $[(\text{TMDAE})\text{Na}(\text{dpa})_2]$, or $[(\text{H}_6\text{-TREN})\text{Na}(\text{dpa})]$ promotes the reactivity of $^t\text{Bu}_2\text{Zn}$ towards the *para*-alkylation of benzophenone. On its own $^t\text{Bu}_2\text{Zn}$ is incapable of such reactivity. In terms of reactivity and selectivity sodium is the best partner for $^t\text{Bu}_2\text{Zn}$, with lithium less selective and potassium unreactive. Different donor ligands also produce *para*-alkylation (1,6-addition) albeit to different extents. This shared selectivity implies a commonality in reaction mechanism though the precise nature of it remains to be established. With both $(\text{Me}_3\text{SiCH}_2)_2\text{Zn}$ and $^t\text{BuLi}$ failing to achieve similar selective alkylations of benzophenone, the scope of the reaction with respect to different alkyl transfer agents would appear limited, though extensions may be possible with other conjugated ketones and other unsaturated substrates. This will be explored in future studies.

Experimental

All reactions were performed under a protective argon atmosphere using standard Schlenk techniques. Hexane, toluene

and THF were dried by heating to reflux over sodium benzo-phenone ketyl and distilled under nitrogen prior to use. $^n\text{BuNa}^{82}$ and $^t\text{Bu}_2\text{Zn}^7$ were prepared according to literature methods. NMR spectroscopy was recorded on a Bruker DPX 400 MHz spectrometer, operating at 400.03 MHz for ^1H and 100.59 MHz for ^{13}C , or a Bruker DPX 500 MHz spectrometer, operating at 500.13 MHz for ^1H and 125.76 MHz for ^{13}C . Dipyrldylamine and benzophenone were purchased from Sigma-Aldrich and were used as received. Single crystal X-ray diffraction measurements were made with Oxford Diffraction instruments and graphite monochromated radiation at 123(2) K. All refinements were against F^2 and to convergence and used programs from the SHELX family.⁸³ Selected crystallographic and refinement details are given in the ESI.†

Preparation of $[(\text{PMDTA})\text{Na}(\text{dpa})]_2$, 2

$M_r = 732.98$ g. $^n\text{BuNa}$ (0.08 g, 1 mmol) was suspended in hexane (15 ml). To this white suspension, dpa(H) (0.17 g, 1 mmol) was added and the resultant suspension was left to stir for 45 minutes. Subsequent addition of PMDTA (0.42 ml, 2 mmol) generated a pale grey solution which, upon transferral to the refrigerator at -30°C , deposited colourless crystalline material after 24 hours [yield 0.30 g; 81% yield based upon the dpa(H) stoichiometry].

δ_{H} (400.03 MHz, d_8 -THF, 300 K) 2.14 [12H, s, $\text{N}(\text{CH}_3)_2$ -PMDTA], 2.18 (3H, s, NCH_3 -PMDTA), 2.42 and 2.31 [4H, t, $^3J_{\text{HH}}$ 7.5 Hz, NCH_2 -PMDTA], 6.20 [2H, ddd, $^3J_{\text{HH}}$ 6.3, 5.0 Hz, $^4J_{\text{HH}}$ 1.5 Hz, H2-dpa], 7.07 [2H, ddd, $^3J_{\text{HH}}$ 8.4 Hz, $^4J_{\text{HH}}$ 1.5 Hz, $^5J_{\text{HH}}$ 1.0 Hz, H4-dpa], 7.14 [2H, ddd, $^3J_{\text{HH}}$ 8.4, 6.3 Hz, $^4J_{\text{HH}}$ 2.0 Hz, H3-dpa], 7.92 [2H, ddd, $^3J_{\text{HH}}$ 5.0 Hz, $^4J_{\text{HH}}$ 2.0 Hz, $^5J_{\text{HH}}$ 1.0 Hz, H1-dpa] ppm. $\delta_{\text{C}\{\text{H}\}}$ (100.59 MHz, C_6D_6 , 300 K) 43.3 (NCH_3 -PMDTA), 46.2 [$\text{N}(\text{CH}_3)_2$ -PMDTA] and, 58.9 and 57.4 (NCH_2 -PMDTA), 110.3 (C2-dpa), 112.5 (C4-dpa), 136.5 (C3-dpa), 149.1 (C1-dpa), 167.2 (C5-dpa) ppm.

Due to the extreme air- and moisture-sensitivity of this compound and compounds 3, 4, and 6, satisfactory elemental microanalysis data could not be obtained.

Crystal data for 2: $\text{C}_{38}\text{H}_{62}\text{N}_{12}\text{Na}_2$, $M_r = 732.98$, triclinic, space group $P\bar{1}$, $a = 10.3495(13)$, $b = 11.0583(11)$, $c = 18.5966(18)$ Å, $\alpha = 101.113(8)$, $\beta = 96.726(9)$, $\gamma = 90.084(9)^\circ$, $V = 2073.4(4)$ Å³, $Z = 2$, $\mu = 0.754$ mm⁻¹. The crystals were treated as twinned with the two parts related by the matrix -0.9813 0.0624 0.0535 0.0681 1.0029 0.0203 -0.1850 -0.5925 -1.0129 . Processing the data gave a *hklf* 5 formatted reflection file with 17 153 reflections. The twin ratio was refined to 0.532(3): 0.468(3). With the aid of restraints on bond lengths and relative displacement parameters, one PMDTA ligand was modelled as disordered over two sites. Final refinement by full-matrix least squares on F^2 gave $R = 0.1510$ (F , 8270 obs. data only) and $R_w = 0.4457$ (F^2 , all data), GOF = 1.167.

Preparation of $[(\text{TMDAE})\text{Na}(\text{dpa})]_2$, 3

$M_r = 706.89$ g. Dpa(H) (0.17 g, 1 mmol) was introduced to a freshly prepared suspension of $^n\text{BuNa}$ (0.08 g, 1 mmol) in hexane (20 ml) and the reaction mixture was stirred for 1 hour. TMDAE (0.38 ml, 2 mmol) was subsequently added *via*

syringe, which produced a yellow solution. Cooling the resultant solution to -30°C for 48 hours afforded a crop of colourless crystals [yield 0.13 g; 37% yield based upon the dpa(H) stoichiometry].

δ_{H} (400.03 MHz, d_8 -THF, 300 K) 2.17 ppm [12H, s, $\text{N}(\text{CH}_3)_2$ -TMDAE], 2.39 (4H, t, $^3J_{\text{HH}}$ 6.1 Hz, NCH_2 -TMDAE), 3.46 (4H, t, $^3J_{\text{HH}}$ 6.1 Hz, OCH_2 -TMDAE), 6.38 [2H, ddd, $^3J_{\text{HH}}$ 6.8, 5.0 Hz, $^4J_{\text{HH}}$ 1.2 Hz, H2-dpa], 7.30 [2H, br. d, $^3J_{\text{HH}}$ 8.4 Hz, H4-dpa] and 7.30 [2H, ddd, $^3J_{\text{HH}}$ 8.4, 6.8 Hz, $^4J_{\text{HH}}$ 2.0 Hz, H3-dpa], 7.99 [2H, ddd, $^3J_{\text{HH}}$ 5.0 Hz, $^4J_{\text{HH}}$ 2.0 Hz, $^5J_{\text{HH}}$ 1.0 Hz, H1-dpa] ppm. $\delta_{\text{C}\{\text{H}\}}$ (100.59 MHz, C_6D_6 , 300 K) 46.3 [$\text{N}(\text{CH}_3)_2$ -TMDAE], 59.9 (NCH_2 -TMDAE), 70.6 (OCH_2 -TMDAE), 112.3 (C2-dpa), 112.6 (C4-dpa), 136.9 (C3-dpa), 148.8 (C1-dpa) and 163.2 (C5-dpa) ppm.

Crystal data for 3: $\text{C}_{36}\text{H}_{56}\text{N}_{10}\text{Na}_2\text{O}_2$, $M_r = 706.89$, orthorhombic, space group $Pbc2_1$, $a = 15.8743(8)$, $b = 12.4146(7)$, $c = 19.8597(11)$ Å, $V = 3913.8(3)$ Å³, $Z = 4$, $\mu = 0.096$ mm⁻¹, 36 891 reflections, 9425 unique, $R_{\text{int}} 0.0617$. With the aid of restraints on bond lengths and relative displacement parameters, one TMDAE ligand was modelled as disordered over two sites. Final refinement by full-matrix least squares on F^2 gave $R = 0.0769$ (F , 6569 obs. data only) and $R_w = 0.2266$ (F^2 , all data), GOF = 1.014.

Preparation of $[(\text{H}_6\text{-TREN})\text{Na}(\text{dpa})]$, 4

$M_r = 339.41$ g. To a freshly prepared suspension of $^n\text{BuNa}$ (0.08 g, 1 mmol) in hexane (15 ml), dpa(H) (0.17 g, 1 mmol) was added and the reaction mixture was allowed to stir for 1 hour. H_6 -TREN (0.15 ml, 1 mmol) was added *via* syringe, followed by toluene (15 ml) with gentle heating to produce a yellow-green solution. Gradual cooling to ambient temperature yielded colourless crystals [yield 0.31 g, 91% yield based upon the dpa(H) stoichiometry]. Despite repeated attempts, efforts to grow X-ray quality crystals of the complex were unsuccessful.

δ_{H} (400.03 MHz, d_8 -THF, 300 K) 1.13 (6H, br. s, NH_2 - H_6 -TREN), 2.40 [6H, t, $^3J_{\text{HH}}$ 6.0 Hz, NCH_2 - H_6 -TREN], 2.65 [6H, t, $^3J_{\text{HH}}$ 6.0 Hz, H_2NCH_2 -TREN], 6.22 [2H, ddd, $^3J_{\text{HH}}$ 8.1, 5.0 Hz, $^4J_{\text{HH}}$ 1.2 Hz, H2-dpa], 7.15 (4H, br. m, H4-dpa and H3-dpa), 7.92 [2H, ddd, $^3J_{\text{HH}}$ 5.0 Hz, $^4J_{\text{HH}}$ 1.8 Hz, $^5J_{\text{HH}}$ 1.3 Hz, H1-dpa] ppm. $\delta_{\text{C}\{\text{H}\}}$ (100.59 MHz, C_6D_6 , 300 K) 41.0 (NCH_2 - H_6 -TREN), 59.1 (NCH_2 - H_6 -TREN), 109.9 (C2-dpa), 113.0 (C4-dpa), 136.2 (C3-dpa), 149.0 (C1-dpa), 167.0 (C5-dpa) ppm.

Preparation of $[\text{Zn}(\text{dpa})_2]$, 6

$M_r = 405.76$ g. Dpa(H) (0.34 g, 2 mmol) was dissolved in a mixed hexane (10 mL)-toluene (20 mL) solvent system. This colourless solution was added to a solution of freshly prepared $\text{Zn}(\text{CH}_2\text{SiMe}_3)_2$ (10 mL of a 0.2 M solution in hexane, 2 mmol). The resultant pale yellow solution deposited a crop of colourless crystals within 24 h [yield 0.08 g; 10% yield based upon the dpa(H) stoichiometry *i.e.*, with a maximum yield of 50%].

Rational synthesis

Dpa(H) (0.34 g, 2 mmol) was dissolved in a mixed toluene (20 mL)-hexane (10 mL) solvent system. This colourless solution was slowly added to a hexane solution of $\text{Zn}(\text{CH}_2\text{SiMe}_3)_2$

(10 mL of a 0.1 M solution in hexane, 1 mmol) *via* syringe. A colourless powder was deposited after 24 h (crude yield 0.33 g, 81%).

Crystal data for **6**: C₂₀H₁₆N₆Zn, *M_r* = 405.76, monoclinic, space group *C2/c*, *a* = 22.5759(4), *b* = 9.5830(2), *c* = 16.0729(3) Å, β = 99.734(2)°, *V* = 3427.23(12) Å³, *Z* = 8, μ = 2.133 mm⁻¹, 10 393 reflections, 3351 unique, *R_{int}* 0.0186, final refinement by full-matrix least squares on *F*² gave *R* = 0.0344 (*F*, 3102 obs. data only) and *R_w* = 0.1000 (*F*², all data), GOF = 1.074.

Unfortunately, the lack of solubility of **6** in common NMR spectroscopic solvents (C₆D₆, *d*₈-THF, *d*₅-pyridine and *d*₆-DMSO) prevented satisfactory NMR spectroscopic analysis from being obtained.

Method A: work-up procedure

To the reaction mixture, deionised water (10 mL), 2 M HCl (20 mL) and diethyl ether (20 mL) were added. The organic layer was separated from the aqueous layer and the aqueous layer was washed with diethyl ether–hexane (3 × 20 mL). Magnesium sulfate was used to dry the combined organic layers. Solvent was removed *in vacuo* and the crude residue was spiked with 10 mol% hexamethylbenzene [0.0162 g, 0.1 mmol for 1 mmol scale (stoichiometric) reactions; 0.081 g, 0.5 mmol for 5 mmol scale (catalytic) reactions]. ¹H NMR spectroscopic analysis was performed in CDCl₃ solvent and the relative yields of 2- and 4-*tert*-butylbenzophenone, benzhydrol⁸³ and diphenyl-*tert*-butylmethanol⁸⁴ were determined by relative integration. Spectroscopic data show resonances that are in good agreement with the reference standard of commercially available samples of 2-*tert*-butylbenzophenone and 4-*tert*-butylbenzophenone.

Control reactions

Stoichiometric conditions: a standard solution of ^tBu₂Zn (2 mL of a 0.5 M solution in hexane, 1 mmol) was transferred to a Schlenk flask under argon atmosphere. A further 6 mL of hexane was added, followed by benzophenone (0.18 g, 1 mmol). The reaction mixture was allowed to stir at ambient temperature for 18 h prior to work-up as per Method A.

Catalytic conditions: a standard solution of ^tBu₂Zn (10 mL of a 0.5 M solution in hexane, 5 mmol) was diluted with a further 30 mL of hexane. Benzophenone (0.90 g, 5 mmol) was added and the reaction mixture was allowed to stir for 18 h under reflux conditions prior to work-up as per Method A.

Variation of donor ligands – stoichiometric conditions

ⁿBuNa (0.16 g, 2 mmol) was suspended in hexane (6 mL) and dpa(H) (0.34 g, 2 mmol) was added. The resultant beige suspension was allowed to stir for 45 minutes at ambient temperature. To this, the donor ligand was injected [DMAP (0.24 g, 2 mmol); TEMPO (0.31 g 2 mmol); TMEDA (0.30 mL, 2 mmol); PMDETA (0.42 mL, 2 mmol); TMDAE (0.38 mL, 2 mmol); H₆-TREN (0.30 mL, 2 mmol); Me₆-TREN (0.42 mL, 2 mmol)]. A hexane solution of ^tBu₂Zn (2 mL of a 0.5 M solution, 1 mmol) was subsequently added, followed by benzophenone (0.18 g, 1 mmol) and the reaction was stirred for 18 h, either at

ambient temperature or at 75 °C (see Table 1) prior to work up according to Method A.

Variation of donor ligands – catalytic conditions

ⁿBuNa (0.08 g, 1 mmol) was suspended in hexane (30 mL) and dpa(H) (0.17 mL, 1 mmol) was added. The reaction mixture was allowed to stir for 45 minutes. Subsequently, the donor ligand was added [DMAP (0.12 g, 1 mmol); TMEDA (0.15 mL, 1 mmol); PMDETA (0.21 mL, 1 mmol); TMDAE (0.14 mL, 1 mmol)]. Following this, ^tBu₂Zn (10 mL of a 0.5 M solution of ^tBu₂Zn in hexane, 5 mmol), and benzophenone (0.90 g, 5 mmol) were added. The reaction mixture was stirred under reflux conditions for 18 h, prior to work-up according to Method A.

Variation of alkali metal – reaction with Lidpa, Nadpa or Kdpa

Following the introduction of an organometallic reagent R'M [R'M = ⁿBuLi (1.25 mL, 1.6 M in hexanes solution, 2 mmol); ⁿBuNa (0.16 g, 2 mmol); or KR (0.25 g, 2 mmol) (where R is CH₂SiMe₃)] to hexane solvent (6 mL), dpa(H) (0.34 g, 2 mmol) was added *via* a solid addition tube. The resultant beige suspension was then stirred for 45 minutes at ambient temperature. To this, PMDETA was injected (0.42 mL, 2 mmol), followed by a hexane solution of ^tBu₂Zn (2 mL of a 0.5 M solution, 1 mmol). Benzophenone (0.18 g, 1 mmol) was subsequently added and the reaction was stirred for 18 hours at ambient temperature. The reaction was worked up following the procedure outlined in Method A.

Variation of solvent – reaction in THF or THF–hexane

ⁿBuNa (0.16 g, 2 mmol) was suspended in hexane (6 mL) and dpa(H) (0.34 g, 2 mmol) was added. The resultant beige suspension was allowed to stir for 45 minutes at ambient temperature, following which, all solvent was removed *in vacuo*. THF (6 mL), TMEDA (0.30 mL, 2 mmol), and ^tBu₂Zn (2 mL of a 0.5 M solution in THF, 1 mmol) were then added.^a Following the addition of benzophenone (0.18 g, 1 mmol), the reaction was allowed to stir at ambient temperature for 18 h, over which time a colour change from orange to green was observed. The reaction was worked up as per Method A. ^aWhen the reaction was performed in a mixed THF–hexane solvent system, hexane (4 mL), TMEDA (0.30 mL, 2 mmol), THF (2 mL) and ^tBu₂Zn (2 mL of a 0.5 M solution in THF, 1 mmol) were injected.

Variation of *tert*-butyl anion source – reaction with ^tBuLi or ^tBu₂Zn

Dpa(H) (0.34 g, 2 mmol) was added to a freshly prepared suspension of ⁿBuNa (0.16 g, 2 mmol) in hexane (6 mL). PMDETA (0.42 mL, 2 mmol) was subsequently introduced, followed by either ^tBu₂Zn (2 mL of a 0.5 M solution in hexane, 1 mmol), or ^tBuLi (1.18 mL of a 1.7 M solution in pentane, 2 mmol). Following the addition of benzophenone (0.18 g, 1 mmol), the reaction was stirred at ambient temperature for 18 hours prior to work up according to Method A.

Variation of R₂Zn

ⁿBuNa (0.16 g, 2 mmol) was suspended in hexane (6 mL) and dpa(H) (0.34 g, 2 mmol) was added. After the reaction mixture was stirred for 1 h, TMEDA (0.30 mL, 2 mmol) was added, followed by R₂Zn (2 mL of a 0.5 M solution in hexane, 1 mmol). Following the addition of benzophenone (0.18 g, 1 mmol), the reaction was allowed to stir for 18 h, either at ambient temperature or under reflux conditions (Table 5) prior to work up according to Method A.

Addition of TEMPO

ⁿBuNa (0.16 g, 2 mmol) was suspended in hexane (6 mL) and dpa(H) (0.34 g, 2 mmol) was added. PMDETA (0.42 mL, 2 mmol) was then injected, followed by ^tBu₂Zn (2 mL of a 0.5 M solution in hexane, 1 mmol). After the addition of benzophenone (0.18 g, 1 mmol) and TEMPO (0.31 g, 2 mmol), the reaction was allowed to stir at ambient temperature for 18 hours prior to work up following the procedure outlined in Method A. ¹H NMR spectroscopic resonances corresponding to TEMPO-^tBu were observed.⁶⁴

δ_{H} (400.03 MHz, CDCl₃, 300 K) 1.10 and 1.15 (6H, s, Me-TEMPO), 1.28 (9H, s, ^tBu), 1.30 (2H, m, γ -TEMPO), 1.48 (4H, m, β -TEMPO) ppm. $\delta_{\text{C}\{\text{H}\}}$ (100.60 MHz, CDCl₃, 300 K) 17.2 (γ -TEMPO), 20.4 (Me-TEMPO), 29.7 (^tBu), 34.8 (Me-TEMPO), 40.9 (β -TEMPO), 59.1 (α -TEMPO), 77.3 (quat. ^tBu) ppm.

Reaction of ^tBu₂Zn and TEMPO

TEMPO (0.16 g, 1 mmol) was added to a hexane (5 mL) solution of ^tBu₂Zn (0.18 g, 1 mmol), upon which the characteristic red-orange colour associated with TEMPO disappeared. After cooling the resultant colourless solution to -30 °C, a crystalline solid, [(TEMPO*)Zn(^tBu)], was deposited after 24 hours (yield 0.08 g; 29%).

δ_{H} (500.13 MHz, C₆D₆, 300 K) 1.18 (12H, s, Me-TEMPO), 1.28 (2H, m, γ -TEMPO), 1.39 (4H, m, β -TEMPO), 1.41 (9H, s, ^tBu) ppm. $\delta_{\text{C}\{\text{H}\}}$ (125.76 MHz, C₆D₆, 300 K) 17.7 (γ -TEMPO), 25.7 (Me-TEMPO), 34.0 (^tBu), and 40.4 (β -TEMPO) ppm.

Due to the extreme air- and moisture-sensitivity of this compound, satisfactory elemental microanalysis data could not be obtained.

Reaction of 2, ^tBu₂Zn and TEMPO

Dpa(H) (0.34 g, 2 mmol) was added to a freshly prepared suspension of ⁿBuNa (0.16 g, 2 mmol) in hexane (8 mL). Subsequently, PMDETA (0.42 mL, 2 mmol), ^tBu₂Zn (2 mL of a 0.5 M solution in hexane, 1 mmol), and TEMPO (0.31 g, 2 mmol) were introduced to the reaction mixture. ¹H and ¹³C{H} NMR spectroscopic data were consistent with those observed for [(TEMPO*)Zn(^tBu)] (*vide supra*).

Reaction of [(TEMPO)Zn(^tBu)] and benzophenone

Following the procedure outlined above on a 3 mmol scale, the stoichiometric combination of ^tBu₂Zn and TEMPO was performed. Crystalline [(TEMPO)Zn(^tBu)] was isolated (0.25 g, 0.9 mmol), dissolved in hexane (8 mL), and benzophenone

(0.18 g, 1 mmol) was added. The reaction mixture was stirred for 18 h at ambient temperature prior to work up as per Method A.

Acknowledgements

This work was generously supported by the UK Engineering and Physical Science Research Council (award no. EP/K001183/1), George Fraser (scholarship award to J.A.G.) and the Royal Society/Wolfson Foundation (research merit award to R.E.M.). We would also like to thank Eva Hevia, Charles T. O'Hara and Stuart D. Robertson for stimulating discussions.

Notes and references

- 1 H. J. Reich, *Chem. Rev.*, 2013, **113**, 7130–7178.
- 2 A. Harrison-Marchand and F. Mongin, *Chem. Rev.*, 2013, **113**, 7470–7562.
- 3 A. Harrison-Marchand and F. Mongin, *Chem. Rev.*, 2013, **113**, 7563–7727.
- 4 R. E. Mulvey and S. D. Robertson, *Angew. Chem., Int. Ed.*, 2013, **52**, 11470–11487.
- 5 B. Haag, M. Mosrin, H. Ila, V. Malakhov and P. Knochel, *Angew. Chem., Int. Ed.*, 2011, **50**, 9794–9824.
- 6 R. E. Mulvey, *Dalton Trans.*, 2013, **42**, 6676–6693.
- 7 P. C. Andrikopoulos, D. R. Armstrong, H. R. L. Barley, W. Clegg, S. H. Dale, E. Hevia, G. W. Honeyman, A. R. Kennedy and R. E. Mulvey, *J. Am. Chem. Soc.*, 2005, **127**, 6184–6185.
- 8 E. Hevia, G. W. Honeyman, A. R. Kennedy and R. E. Mulvey, *J. Am. Chem. Soc.*, 2005, **127**, 13106–13107.
- 9 D. R. Armstrong, J. A. Garden, A. R. Kennedy, S. M. Leenhouts, R. E. Mulvey, P. O'Keefe, C. T. O'Hara and A. Steven, *Chem. – Eur. J.*, 2013, **19**, 13492–13503.
- 10 A. R. Kennedy, R. E. Mulvey and R. B. Rowlings, *J. Am. Chem. Soc.*, 1998, **120**, 7816–7824.
- 11 P. García-Álvarez, D. V. Graham, E. Hevia, A. R. Kennedy, J. Klett, R. E. Mulvey, C. T. O'Hara and S. Weatherstone, *Angew. Chem., Int. Ed.*, 2008, **47**, 8079–8081.
- 12 E. Crosbie, P. Garcia-Alvarez, A. R. Kennedy, J. Klett, R. E. Mulvey and S. D. Robertson, *Angew. Chem., Int. Ed.*, 2010, **49**, 9388–9391.
- 13 R. Campbell, E. Crosbie, A. R. Kennedy, R. E. Mulvey, R. A. Naismith and S. D. Robertson, *Aust. J. Chem.*, 2013, **66**, 1189–1201.
- 14 J. M. L'Helgoual'ch, G. Bentabed-Ababsa, F. Chevallier, M. Yonehara, M. Uchiyama, A. Derdour and F. Mongin, *Chem. Commun.*, 2008, 5375–5377.
- 15 K. Snegaroff, J. M. L'Helgoual'ch, G. Bentabed-Ababsa, T. T. Nguyen, F. Chevallier, M. Yonehara, M. Uchiyama, A. Derdour and F. Mongin, *Chem. – Eur. J.*, 2009, **15**, 10280–10290.

- 16 D. R. Armstrong, A. R. Kennedy, R. E. Mulvey, J. A. Parkinson and S. D. Robertson, *Chem. Sci.*, 2012, **3**, 2700–2707.
- 17 B. D. Murray and P. P. Power, *Inorg. Chem.*, 1984, **23**, 4584–4588.
- 18 J. Garcia-Álvarez, A. R. Kennedy, J. Klett and R. E. Mulvey, *Angew. Chem., Int. Ed.*, 2007, **46**, 1105–1108.
- 19 M. Hatano, T. Matsumura and K. Ishihara, *Org. Lett.*, 2005, **7**, 573–576.
- 20 M. Hatano, S. Suzuki and K. Ishihara, *J. Am. Chem. Soc.*, 2006, **128**, 9998–9999.
- 21 M. Hatano and K. Ishihara, *Synthesis*, 2008, 1647–1675.
- 22 M. Hatano, S. Suzuki and K. Ishihara, *Synlett*, 2010, 321–324.
- 23 J. J. Crawford, B. J. Fleming, A. R. Kennedy, J. Klett, C. T. O'Hara and S. A. Orr, *Chem. Commun.*, 2011, **47**, 3772–3774.
- 24 D. R. Armstrong, J. A. Garden, A. R. Kennedy, R. E. Mulvey and S. D. Robertson, *Angew. Chem., Int. Ed.*, 2013, **52**, 7190–7193.
- 25 K. Gregory, P. v. R. Schleyer and R. Snaith, *Adv. Inorg. Chem.*, 1991, **37**, 47–142.
- 26 D. Barr, W. Clegg, L. Cowton, L. Horsburgh, F. M. Mackenzie and R. E. Mulvey, *J. Chem. Soc., Chem. Commun.*, 1995, 891–892.
- 27 I. Cragg-Hine, M. G. Davidson, A. J. Edwards, P. R. Raithby and R. Snaith, *J. Chem. Soc., Dalton Trans.*, 1994, 2901–2902.
- 28 A. R. Kennedy, J. Klett, C. T. O'Hara, R. E. Mulvey and G. M. Robertson, *Eur. J. Inorg. Chem.*, 2009, 5029–5035.
- 29 J. A. Garden, A. R. Kennedy, R. E. Mulvey and S. D. Robertson, *Dalton Trans.*, 2011, **40**, 11945–11954.
- 30 M. Karl, G. Seybert, W. Massa, K. Harms, S. Agarwal, R. Maleika, W. Stelter, A. Greiner, W. H. B. Neumüller and K. Dehnicke, *Z. Anorg. Allg. Chem.*, 1999, **625**, 1301–1309.
- 31 F. H. Allen, Search performed 06/01/14, Version 1.15, *Acta Crystallogr. Sect. B: Struct. Sci.*, 2002, **58**, 380–388.
- 32 P. C. Andrews, W. Clegg and R. E. Mulvey, *Angew. Chem., Int. Ed. Engl.*, 1990, **29**, 1440–1441.
- 33 D. R. Armstrong, W. Clegg, R. P. Davies, S. T. Liddle, D. J. Linton, P. R. Raithby, R. Snaith and A. E. H. Wheatley, *Angew. Chem., Int. Ed.*, 1999, **38**, 3367–3370.
- 34 S. T. Liddle and W. Clegg, *Polyhedron*, 2003, **22**, 3507–3513.
- 35 W. Clegg and S. T. Liddle, *Acta Crystallogr., Sect. E: Struct. Rep. Online*, 2004, **60**, 1492–1494.
- 36 S. T. Liddle and W. Clegg, *J. Chem. Soc., Dalton Trans.*, 2001, 402–408.
- 37 S. T. Liddle and W. Clegg, *Polyhedron*, 2002, **21**, 2451–2455.
- 38 S. T. Liddle, W. Clegg and C. A. Morrison, *Dalton Trans.*, 2004, 2514–2525.
- 39 J. R. Allan, G. M. Baillie, L. A. Macindoe, A. J. Blake, H. J. Bowley and D. L. Gerrard, *Acta Crystallogr., Sect. C: Cryst. Struct. Commun.*, 1988, **44**, 1833–1834.
- 40 W. Kohn, A. D. Becke and R. G. Parr, *J. Phys. Chem.*, 1996, **100**, 12974–12980.
- 41 A. D. McLean and G. S. Chandler, *J. Chem. Phys.*, 1980, **72**, 5639–5648.
- 42 J. H. N. Buttery, N. C. Plackett, B. W. Skelton, C. R. Whitaker and A. H. White, *Z. Anorg. Allg. Chem.*, 2006, **632**, 1856–1869.
- 43 D. M. Cousins, M. G. Davidson, C. J. Frankis, D. García-Vivó and M. F. Mahon, *Dalton Trans.*, 2010, **39**, 8278–8280.
- 44 M. G. Davidson, D. García-Vivó, A. R. Kennedy, R. E. Mulvey and S. D. Robertson, *Chem. – Eur. J.*, 2011, **17**, 3364–3369.
- 45 A. R. Kennedy, R. E. Mulvey, C. T. O'Hara, G. M. Robertson and S. D. Robertson, *Angew. Chem., Int. Ed.*, 2011, **50**, 8525–8528.
- 46 D. R. Armstrong, M. G. Davidson, D. García-Vivó, A. R. Kennedy, R. E. Mulvey and S. D. Robertson, *Inorg. Chem.*, 2013, **52**, 12023–12032.
- 47 N. D. R. Barnett, R. E. Mulvey, W. Clegg and P. A. O'Neil, *J. Am. Chem. Soc.*, 1993, **115**, 1573–1574.
- 48 M. A. Nichols and P. G. Williard, *J. Am. Chem. Soc.*, 1993, **115**, 1568–1572.
- 49 T. Stey and D. Stalke, *The Chemistry of Organolithium Compounds*, John Wiley and Sons, Ltd, Chichester, 2004.
- 50 V. H. Gessner, C. Daschlein and C. Strohmman, *Chem. – Eur. J.*, 2009, **15**, 3320–3334.
- 51 M. D. Rausch and D. J. Ciappenelli, *J. Organomet. Chem.*, 1967, **10**, 127–136.
- 52 D. B. Collum, *Acc. Chem. Res.*, 1992, **25**, 448–454.
- 53 D. B. Collum, *Acc. Chem. Res.*, 1993, **26**, 227–234.
- 54 J. F. Remenar, B. L. Lucht, D. Kruglyak, F. E. Romesburg, J. H. Gilchirst and D. B. Collum, *J. Org. Chem.*, 1997, **62**, 5748–5754.
- 55 H. Oulyadi, C. Fressigné, Y. Yuan, J. Maddaluno and A. Harrison-Marchand, *Organometallics*, 2012, **31**, 4801–4809.
- 56 A. Corruble, J.-Y. Valnot, J. Maddaluno, Y. Prigent, D. Davoust and P. Duhamel, *J. Am. Chem. Soc.*, 1997, **119**, 10042–10048.
- 57 K. Maruyama, Y. Matano and T. Katagiri, *J. Phys. Org. Chem.*, 1991, **4**, 501–519.
- 58 A. R. Kennedy, J. Klett, R. E. Mulvey and D. S. Wright, *Science*, 2009, **326**, 706–708.
- 59 A. Fürstner and G. Seidel, *Tetrahedron*, 1995, **51**, 11165–11176.
- 60 H. Takahashi, K. M. Hossain, Y. Nishihara, T. Shibata and K. Takagi, *J. Org. Chem.*, 2006, **71**, 671–675.
- 61 D. C. Nonhebel and J. C. Walton, *Free Radical Chemistry*, Cambridge University Press, New York, 1974.
- 62 G. C. Forbes, A. R. Kennedy, R. E. Mulvey and P. J. A. Rodger, *Chem. Commun.*, 2001, 1400–1401.
- 63 L. Balloch, A. M. Drummond, P. García-Alvarez, D. V. Graham, A. R. Kennedy, J. Klett, R. E. Mulvey, C. T. O'Hara, P. J. A. Rodger and I. D. Rushworth, *Inorg. Chem.*, 2009, **48**, 6934–6944.
- 64 T. Vogler and A. Studer, *Synthesis*, 2008, 1979–1993.
- 65 D. R. Armstrong, L. Balloch, J. J. Crawford, B. J. Fleming, L. M. Hogg, A. R. Kennedy, J. Klett, R. E. Mulvey, C. T. O'Hara, S. A. Orr and S. D. Robertson, *Chem. Commun.*, 2012, **48**, 1541–1543.

- 66 G. Sorin, R. M. Mallorquin, Y. Contie, A. Baralle, M. Malacria, J. P. Goddard and L. Fensterbank, *Angew. Chem., Int. Ed.*, 2010, **49**, 8721–8723.
- 67 T. Holm and I. Crossland, *Acta Chem. Scand.*, 1971, **25**, 59–69.
- 68 C. C. L. Thum, G. N. Khairallah and R. A. J. O'Hair, *Angew. Chem., Int. Ed.*, 2008, **47**, 9118–9121.
- 69 C. Blomberg, R. M. Salinger and H. S. Mosher, *J. Org. Chem.*, 1969, **34**, 2385–2388.
- 70 E. C. Ashby and J. J. R. Bowers, *J. Am. Chem. Soc.*, 1981, **103**, 2242–2250.
- 71 A. Grirrane, I. Resa, A. Rodríguez, E. Carmona, E. Alvarez, E. Gutiérrez-Puebla, A. Monge, A. Galindo, D. del Río and R. A. Andersen, *J. Am. Chem. Soc.*, 2007, **129**, 693–703.
- 72 M. H. Dickman and R. J. Doedens, *Inorg. Chem.*, 1982, **21**, 682–684.
- 73 P. Jaitner, W. Huber, G. Hunter and O. Scheidsteger, *J. Organomet. Chem.*, 1983, **259**, C1–C5.
- 74 J. Laugier, J. M. Latour, A. Caneschi and P. Rey, *Inorg. Chem.*, 1991, **30**, 4474–4477.
- 75 M. K. Mahanthappa, K. W. Huang, A. P. Cole and R. M. Waymouth, *Chem. Commun.*, 2002, 502–503.
- 76 D. J. Mindiola, R. Waterman, D. M. Jenkins and G. L. Hillhouse, *Inorg. Chim. Acta*, 2003, **345**, 299–308.
- 77 T. Iwamoto, H. Masuda, S. Ishida, C. Kabuto and M. Kira, *J. Am. Chem. Soc.*, 2003, **125**, 9300–9301.
- 78 A. Naka, N. J. Hill and R. West, *Organometallics*, 2004, **23**, 6330–6332.
- 79 G. H. Spikes, Y. Peng, J. C. Fetting, J. Steiner and P. P. Power, *Chem. Commun.*, 2005, 6041–6043.
- 80 C. Jones and R. P. Rose, *New J. Chem.*, 2007, **31**, 1484–1487.
- 81 W. J. Evans, J. M. Perotti, R. J. Doedens and J. W. Ziller, *Chem. Commun.*, 2001, 2326–2327.
- 82 C. Schade, W. Bauer and P. v. R. Schleyer, *J. Organomet. Chem.*, 1985, **295**, 25–28.
- 83 G. M. Sheldrick, *Acta Crystallogr., Sect. A: Fundam. Crystallogr.*, 2008, **64**, 112–122.
- 84 N. J. Findlay, S. R. Park, F. Schoenebeck, E. Cahard, S. Zhou, L. E. A. Berlouis, M. D. Spicer, T. Tuttle and J. A. Murphy, *J. Am. Chem. Soc.*, 2010, **132**, 15462–15464.